Eur. Phys. J. C 21, 557–562 (2001)
Digital Object Identifier (DOI) 10.1007/s100520100743

THE EUROPEAN PHYSICAL JOURNAL C

Chaotic sources and percolation of strings in heavy ion collisions

M.A. Braun[1], F. del Moral[2], C. Pajares[2]

[1] High-energy department, St. Petersburg University, 198904 St. Petersburg, Russia
[2] Departamento de Física de Partículas, Universidade de Santiago de Compostela, 15706 Santiago de Compostela, Spain

Received: 19 February 2001 / Revised version: 5 July 2001 /
Published online: 10 August 2001 –

Abstract. The chaoticity parameter λ of Bose–Einstein correlations is studied as a tool for analyzing the interaction between color strings in multiparticle production at high energies. Different scenarios of this interaction lead to a different behavior of λ with energy and atomic number of the participants. Comparison to the present experimental data favors the percolation of strings scenario. The one of its versions in which λ shows a peculiar dependence on the string density, very similar to the dependence of the fractional average cluster size, looks particularly attractive.

1 Introduction

Originating in astronomy, the Hanbury–Brown–Twiss (HBT) effect [1] allows one to obtain information about the structure of the emitting source using the Bose–Einstein correlations (BEC) between the momenta of two identical particles. It has lately been widely used in high energy multiparticle production [2–6]. At present, BEC represent the only viable way to know the space-time extension of the production region [3]. The correlation function is given by [5]

$$C_2(p_1^\mu, p_2^\mu) = \frac{\rho(p_1^\mu, p_2^\mu)}{\rho(p_1^\mu)\rho(p_2^\mu)}, \tag{1.1}$$

where the ρ's are the corresponding two and one particle inclusive cross sections. Different parameterizations have been used for C_2, for instance [7]

$$C_2(q) = 1 + \lambda \exp[-R_{\mathrm{T}}^2 q_{\mathrm{T}}^2 - R_\parallel^2 (q_{\mathrm{L}}^2 - q_0^2) - (R_0^2 + R_\parallel^2)\gamma^2 (q_0^2 - v q_z^2)], \tag{1.2}$$

$$q^\mu = p_1^\mu - p_2^\mu, \quad \gamma = 1/\sqrt{1-v^2}. \tag{1.3}$$

In all the parameterizations, the parameter

$$\lambda \equiv C_2(q=0) - 1 \tag{1.4}$$

measures the correlation strength. It can also be interpreted as a measure of chaoticity, or degree of coherence, of the reaction and is known under this name [8,9]. $\lambda = 0$ or 1 correspond to a totally coherent or totally chaotic emission of secondaries, respectively.

Most of the papers related to BEC in the search of the quark gluon plasma (QGP) study the size parameters of the correlation function. In this paper, we study the chaoticity parameter λ. We find that it also carries substantial information about the dynamics of the multiparticle production and in particular of the possible formation of QGP.

As in most of the models of soft hadronic interactions, we assume that color strings are formed between the projectile and target during the collision, which break due to the formation of quark–antidiquark or diquark–antidiquark pairs. These strings are of the Lund type, and therefore correspond to totally chaotic sources, $\lambda = 1$ [10–12]. For particles coming from different strings we assume absence of BEC; that is, $\lambda = 0$. This assumption is usually done in the framework of the Lund model [13]. We are aware that the justification of this assumption is not clear at all [14]. In fact, the corresponding 4 to 4 amplitude, obtained via the generalized optical theorem, should be symmetrized if the two particles are identical, irrespective of whether the two particles are emitted in the same string or in two different ones. This second possibility can give leading contributions in AB [15]. The studies of W^+W^- events produced in e^+e^- collisions can provide some experimental information on the problem. BEC's are consistent with the picture where pions from the W system are unaware of the pions produced by the others [16,17]. Also the drop of λ with multiplicity observed by UA1 is consistent with our assumption.

Under these assumptions one finds that [18]

$$\lambda = \frac{n_{\mathrm{S}}}{n_{\mathrm{T}}}, \tag{1.5}$$

where n_{S} is a mean number of particle pairs produced in a given rapidity and transverse momentum range in the same string and n_{T} is a mean total number of pairs produced in the same kinematical range.

From (1.5) it is clear, that $\lambda = 1$ for a single string and decreases with the increasing number of independent

strings. Therefore λ, in a sense, measures the mean number of effective strings (sources) existing in a given collision [19–21].

It is important to realize that strings cannot be pointlike in the transverse space. Each string should have a finite transverse dimension, determined by the color field stretched between the color charges of the partons placed at the extremes of the strings. As the energy and/or atomic number of the projectile and target increase the number and density of strings also increase, so that the strings start to overlap in the transverse space. What really happens when strings overlap, that is, how they interact at close distance, is a dynamical question. Two possible limiting scenarios have been proposed on the subject. One may assume that overlapping strings immediately fuse into a new string with a higher color, like drops of liquid. This evidently means an abrupt change of the color field geometry as soon as the strings touch each other. In an alternative smooth scenario one may think that the geometrical structure of the color field does not change: the strings preserve their individual form in the transverse space and only the color field becomes stronger in the cluster region. The dynamical properties of the strings are very different in these two scenarios. In particular, in the first, "fusion" scenario there is no phase transition as the string density grows indefinitely. To the contrary, in the second scenario the percolation phase transition occurs as the density grows up to a certain critical one. We call this latter scenario the "percolation" one. We have no theoretical preferences for either of these scenarios and hope that the experimendal evidence will give the possibility to choose between them (or reject both). Unfortunately for global observables, such as multiplicities or transverse momentum distributions, most of the predictions are rather similar in both models.

In this paper, we show how the existing and forthcoming experimental data on the chaoticity parameter λ can distinguish between these two possibilities. In particular, we show that in the percolation scenario the behavior of λ with the energy and atomic number of the projectile and target is in agreement with the general trend of experimental data. Previously, similar research was done pointing out that the general trend of the data could be explained by a possible onset of collective phenomena [18]. These collective phenomena seem to reduce drastically the effective number of strings. Here we go further, showing that this collective behavior is very probably realized by percolation of strings.

The plan of this paper is as follows. First the experimental situation is summarized in Sect. 2. In the next two sections we compute the chaoticity parameter in different scenarios of string interaction. Finally our conclusions are presented in Sect. 5.

2 Experimental data

The experimental data on λ have been obtained in very different kinematical situations and also assuming different extrapolations and corrections, which makes rather difficult the comparison with theoretical models and even the comparison among the different data.

Data with light projectiles like hadrons or oxygen [20, 22] show that λ decreases as the multiplicity or the atomic number of the target increases. For instance, the values of λ for O–C, O–Cu, O–Ag and O–Au [22] are 0.92 ± 0.1, 0.29 ± 0.03, 0.22 ± 0.03 and 0.160 ± 0.006, respectively. These numbers correspond to a centrality, characterized by the average number of the participants quoted as equal to 19.2, 39.5, 47.2 and 52.9 respectively. The rapidity range considered was $-1 \leq y_{\rm lab} \leq 1$. The same experiment shows a somewhat weaker decrease for p, O and S colliding with the Au target: $\lambda = 0.45 \pm 0.08$, 0.32 ± 0.04 and 0.33 ± 0.04, respectively [23]. NA44 quoted a value of 0.56 ± 0.02 for S–Pb central collisions (3% most central collisions) and 0.59 ± 0.03 for Pb–Pb central collisions (15% centrality) [24]. The range of pseudorapidity is $1.8 < \eta < 3.3$ and $p_{\rm T} = 150\,{\rm MeV}/c$ and $170\,{\rm MeV}/c$ respectively. In a different kinematics, $3.1 < y < 4.3$, the forward rapidity region, NA44 obtains $\lambda = 0.46 \pm 0.04$ for S–Pb [25].

As we see, the experimental situation on λ is not clear but some trends can be distinguished. First, a decrease of λ with the growth of multiplicity for a small number of collisions is observed, as the data with p and O projectiles show. As the number of collisions goes up, the behavior of λ changes: it no longer decreases with the multiplicity and even may increase, as the central Pb–Pb collisions data show. Also the values of λ found at the edge of the rapidity range are larger than the ones measured in the central rapidity region. (Notice that the pion multiplicity is larger in the central rapidity region.)

In the comparison of theory and experiment attention has to be paid to the normalization of the correlation function. Instead of using the denominator in (1.1), that is, the product of the single inclusive cross sections for each particle, in the experimental data a background spectrum $B(p_1^\mu, p_2^\mu)$ is usually used to exclude all such effects as production dynamics, experimental acceptances and biases, leaving only those induced by BEC. The most common prescription for $B(p_1^\mu, p_2^\mu)$ is that of different-event mixing. In this scheme, events combining individual pions taken from different events are used to calculate the background spectrum. Details on that can be found in [25, 26]. Equation (1.5) has been obtained without taking into account a possible enhancement due to Bose–Einstein statistics in the single inclusive cross sections, which is essentially equivalent to using the same normalization in the experiments under the same kinematical conditions. Therefore, to obtain the true correlation function and the λ parameter the experimentalists have to correct the obtained value. Following the NA44 collaboration one writes

$$\lambda = K_{\rm spc}(p_1, p_1)(\lambda_{\rm uc} + 1) - 1, \tag{2.1}$$

where $\lambda_{\rm uc}$ and λ are the uncorrected and corrected chaoticity parameters, respectively and $K_{\rm spc}(k, k)$ is a correction to the normalization, that is, to the product of the single inclusive cross sections. In our calculations we correct our values using formula (2.1).

Another point which should be mentioned is that λ depends on the sum of the momenta of the particles (always at $\boldsymbol{p}_1 = \boldsymbol{p}_2$). In the rest of the paper we do not take into account this dependence, since we consider only low momenta ($\boldsymbol{p}_1 \approx 0$). The above mentioned experimental λ's also correspond to low momenta.

Finally, we consider only prompt particles. Particles coming from long-lived resonances are produced coherently so that some partial degree of coherence has to be introduced into the decay of Lund strings [27]. This would reduce the λ value. To take into account this effect a very sophisticated Monte-Carlo code is needed. As we are interested only in the general trend and not in the detailed comparison, we neglect this effect.

3 String fusion

In the fusion of strings [28] or in the formation of color ropes [29], strings fuse as soon as their transverse positions come within a certain interaction area: of the order of the string transverse dimension πr^2. The fusion of strings may take place only when their rapidity intervals overlap. The emerging string has the energy-momentum equal to the sum of the energy-momenta of the original strings and the same transverse size πr^2. Its color properties are determined from the standard SU(3) color composition law.

Using the analytical version of the string fusion model [30,31], the probability of obtaining ν_n clusters formed from n original strings is

$$P(\nu_n) = \frac{cp^{N-M}}{\prod_{n=1}(\nu_n!(n!)^{\nu_n})} \prod_{k=1}^{M-1}(1-kp), \tag{3.1}$$

where c is a normalization constant, p the fusion probability, N the total number of strings and M the total number of clusters

$$p = r^2/R^2, \quad M = \sum_n \nu_n, \quad N = \sum_n n\nu_n \tag{3.2}$$

(πR^2 is the total interaction area). The mean value of the number of clusters with n fused strings is

$$\langle \nu_n \rangle = C_N^n p^{n-1}(1-p)^{N-n}, \tag{3.3}$$

and therefore

$$\langle M \rangle = \frac{1}{p}\left(1-(1-p)^N\right). \tag{3.4}$$

In the "thermodynamical limit" $p \to 0$, $N \to \infty$, the relevant parameter is the string density $\eta = Np = Nr^2/R^2$. In this limit the ratio

$$\frac{\langle M \rangle}{N} = \frac{1}{\eta}(1-\mathrm{e}^{-\eta}) = F^2(\eta) \tag{3.5}$$

depends only on η.

The multiplicity μ_n of a cluster of n strings is proportional to the color charge at its ends [28,29]. Since the color charge of the cluster is a vectorial sum of the color charges of fusing strings, we find

$$\langle Q_n^2 \rangle = n\langle Q_1^2 \rangle, \tag{3.6}$$

where Q_1 is the color charge of the single string and we have used the fact that the average of the product of color charges of different strings is zero.

From this we conclude

$$\mu_n = \sqrt{n}\mu_1. \tag{3.7}$$

Turning to (1.5) and using the results of [31] we find

$$n_{\mathrm{S}} = \frac{1}{2}\left\langle \sum_{n=1}^{N} \nu_n \sqrt{n}\mu_1 \left(\sqrt{n}\mu_1 - 1\right) \right\rangle, \tag{3.8}$$

$$n_{\mathrm{T}} = \frac{1}{2}\left\langle \left(\sum_{n=1}^{N} \nu_n \sqrt{n}\mu_1\right)\left(\sum_{n=1}^{N} \nu_n \sqrt{n}\mu_1 - 1\right) \right\rangle. \tag{3.9}$$

It follows that

$$\lambda = \frac{1}{NF(\eta)^2}. \tag{3.10}$$

For low η, λ falls with N as expected because this case corresponds to independent strings. At large η, λ results independent of N. In this limit $\lambda = r^2/R^2$. The experimental data agree qualitatively with such a behavior but already at η slightly above one (Pb–Pb central collisions at SPS energies) λ begins to grow. In addition to this, for Pb–Pb, the values of λ are not so small as r^2/R^2. So we conclude that the fusion scenario seems to contradict the experimental data.

4 Percolation of strings

As mentioned, in the case of string fusion there is no phase transition so far as the formed clusters have the same size as the original strings [31]. In an alternative scenario the area of a cluster is formed by the geometrical sum of overlapping strings areas. In this case the percolation phase transition takes place when η reaches a critical value, η_c [32]. It corresponds to the appearance of at least one path formed by overlapping strings which passes through the whole transverse area of the interaction. The value of η_c lies in the interval 1.17–1.5, depending on the profile functions used for the colliding nuclei [33].

In the percolation scenario the dynamics of string interaction may in principle be of different forms. We are going to considerer three cases:

(a) The color field is summed only in the overlapping region of the original strings [34]. In the rest of the area the field does not change. As a result, the cluster behaves in general as several independent sources, their number depending on the way of overlapping.
(b) The resulting color field is spread homogeneously all over the cluster area. Then each cluster can be considered as a single source of incoherent (chaotic) production of particles.

(c) An intermediate situation between the cases (a) and (b). Each cluster is considered as a single source like in (b) and also the color is assumed homogeneous all over the cluster but this color is given by a vectorial sum of the original strings times a factor which takes into account the ratio between the area of the cluster and the area of the original strings. In this way the abrupt change of the field strength is avoided which occurs in case (b) when strings overlap in a small area. In case (c) the number of particles produced by clusters of the same number of strings but overlapping differently is different.

Let us start with the case (a). Denote by n_i the numbers of regions where i strings overlap and by S_{ij} the area of the jth such region. Then $S_i = \sum_{j=1}^{n_i} S_{ij}$ is the total area where i strings overlap.

The color of the jth region where i strings overlap is $i^{1/2}S_{ij}Q_1/S_1$ and the multiplicity of the particles produced in this region will be $i^{1/2}S_{ij}\mu_1/S_1$. Therefore

$$n_{\mathrm{S}} = \frac{1}{2}\mu_1^2 \left\langle \sum_{i=1}^{N}\sum_{j=1}^{n_i} i S_{ij}^2/S_1^2 \right\rangle, \tag{4.1}$$

$$n_{\mathrm{T}} = \frac{1}{2}\mu_1^2 \left\langle \left(\sum_{i=1}^{N} \sqrt{i} S_i/S_1 \right)^2 \right\rangle. \tag{4.2}$$

Using the results of [34], we obtain in the thermodynamical limit

$$\lambda = \frac{I}{NG(\eta)^2}, \tag{4.3}$$

where [34]

$$I = \int_0^2 \mathrm{d}R R \frac{2}{\pi}(\alpha - \sin\alpha)\mathrm{e}^{-2\eta[1-(1/\pi)(\alpha-\sin\alpha)]}, \tag{4.4}$$

$$G(\eta) = \sum_{n=1}^{\infty} \sqrt{n}\frac{\eta^n}{n!}\mathrm{e}^{-\eta} \simeq \sqrt{\frac{1-\mathrm{e}^{-\eta}}{\eta}} = F(\eta) \tag{4.5}$$

and $\alpha = 2\arccos(R/2)$.

Since the multiplicity is

$$\mu = N\mu_1 F(\eta), \tag{4.6}$$

the quantity

$$\frac{\lambda\mu}{\mu_1} = \frac{I}{F(\eta)} \tag{4.7}$$

depends only on η.

For small η, $\lambda \sim I/N$ and falls with N as in the string fusion scenario. However for large η, $\lambda \to 0$ in clear disagreement with the trend of the experimental data.

Now we pass to the case (b), where every cluster of overlapping strings acts like a chaotic source. If the cluster has i strings its color is $Q_i = i^{1/2}Q_1$ and therefore the multiplicity from this cluster is

$$\mu_i = \sqrt{i}\mu_1. \tag{4.8}$$

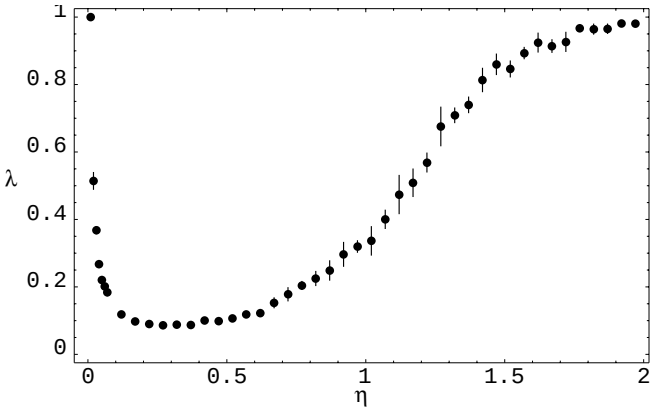

Fig. 1. Dependence of λ on η for percolating strings in case (b) of the text according to formula (4.11)

The number of pairs of identical particles produced by the cluster is

$$n_{\mathrm{S}} = \frac{1}{2}\mu_1^2 \left\langle \sum_{n=1}^{N} \nu_n n \right\rangle, \tag{4.9}$$

and the total number of pair of identical particles produced is

$$n_{\mathrm{T}} = \frac{1}{2}\mu_1^2 \left\langle \left(\sum_{n=1}^{N} \nu_n \sqrt{n} \right)^2 \right\rangle. \tag{4.10}$$

So we find

$$\lambda = \frac{N}{\left\langle \left(\sum_{n=1}^{N} \nu_n \sqrt{n} \right)^2 \right\rangle} \tag{4.11}$$

To compute (4.11) a Monte-Carlo simulation was done, generating N circles of radius r inside a circle of radius R. Varying N with r and R and fixed, we obtained the dependence of λ on η which is shown in Fig. 1. The error bars at each η correspond to statistical errors of our simulation. They are larger at higher η because we generated less events.

The obtained results are in agreement with the general trend of the experimental data. For $\eta > 0.4$ the peculiar dependence of λ on the string density that we found is very similar to the dependence of the fractional average cluster size [35]. Also, the derivative of the string density is maximal at the critical point.

More realistic calculations, taking into account the energy-momentum of the strings and of the clusters, were done by a Monte-Carlo simulation with the following ingredients:

(1) We generated configurations of strings in the transverse space for different nucleus–nucleus collisions. The wave functions of the nuclei and the distribution of the partons in the nucleon were taken standard [28]. Each string had its energy-momentum specified by the energy-momentum of the partons at the ends, given by the corresponding structure functions. Up to this point we followed the code described in [28].

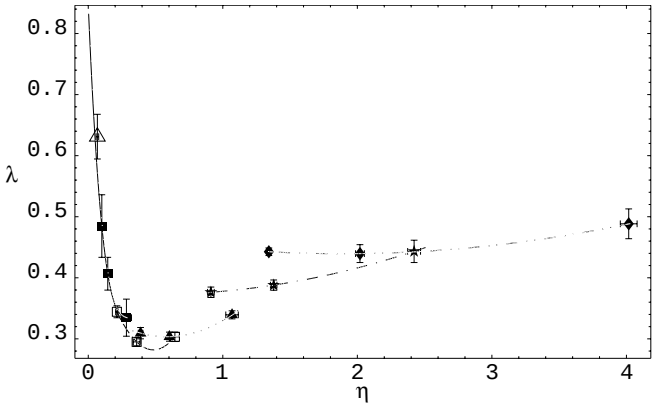

Fig. 2. Dependence of λ on η for different nucleus–nucleus collisions with percolating strings in case (b) of the text taking into account the energy-momentum of the strings. Each point represents a specific type of nucleus–nucleus collisions explained in the text. Correlations are calculated between identical pions for $y_{1\mathrm{cm}} = y_{2\mathrm{cm}} = 0.5$ and $m_{\mathrm{T}_1} = m_{\mathrm{T}_2} = 0.35\,\mathrm{GeV}/c^2$

(2) We identified clusters from the known transverse positions of the strings. Each cluster was given an energy-momentum equal to the sum of the energy-momenta of the strings which form it. Its color was taken as $n^{1/2}$ if it is formed of n strings.
(3) A cluster of n strings of energy E_j was assumed to produce a number of particles

$$\mu_n = \sqrt{n}\mu_1(E), \tag{4.12}$$

where $E = \sum_{j=1}^{n} E_j$ and $\mu_1(E)$ is the multiplicity of a single string depending on the energy, which is known [28].

In this way, we calculated the ratio $n_{\mathrm{S}}/n_{\mathrm{T}}$ to obtain the curve presented in Fig. 2, where the points are the results, from left to right, for C–C minimum bias collisions at SPS energies (non-filled triangles), S–S minimum bias collisions at SPS, RHIC ($s^{1/2} = 200\,\mathrm{GeV}$ A) and LHC ($s^{1/2} = 5500\,\mathrm{GeV}$ A) energies respectively (filled boxes), O–O central collisions at SPS, RHIC and LHC energies respectively (non-filled boxes), S–S central collisions at SPS, RHIC and LHC energies respectively (filled triangles), Ag–Ag central collisions at SPS, RHIC and LHC energies respectively (stars) and Pb–Pb central collisions at SPS, RHIC and LHC energies respectively (diamonds).

Each point was obtained by the simulation of events which produce particles in the central rapidity region coming from the fragmentation of clusters formed from a number N original strings, which was determined by the type of collision. As this type also determines the total transverse area of the interaction, the corresponding value of η was also fixed. The vertical error bars correspond to the statistics of the simulation, and the horizontal bars correspond to the uncertainties in N for a given type of collisions.

We observe that the results do not depend only on η but also on A, so that the η scaling is broken. For high η the values of λ are lower than the ones corresponding to Fig. 1. In any case, the results reproduce rather well the general trend of the experimental data.

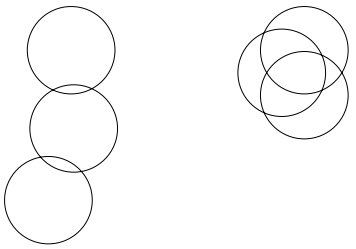

Fig. 3. Two clusters formed from three strings with very little and very large overlapping

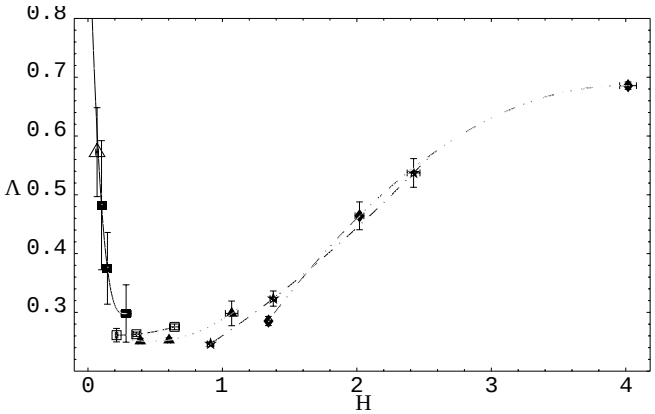

Fig. 4. Dependence of λ on η for percolating strings in case (c) of the text taking into account the energy-momentum of the strings. The points correspond to the same type of collisions as in Fig. 2

Finally we discuss case (c). In Fig. 3 we show two different clusters of three strings. In the previous case, the color extended all over the whole area is the same for both clusters, equal to $3^{1/2}Q_1$. This looks unphysical and the effect of the different total areas should be taken into account. For this reason we assign color $(3A_3/A_1)^{1/2}Q_1$ to the cluster, where A_3 is the area of the cluster and A_1 is the area of a single string. Then if the three strings are just touching each other the assigned color is $(3{\cdot}3)^{1/2}Q_1 = 3Q_1$ and there is no color suppression, so that the cluster gives the same multiplicity as three independent strings. In the other extreme case, when the three strings are fully overlapping, the color is $(3 \cdot 1)^{1/2}Q_1$, and we find a maximal color suppression, as in cases (a) and (b) discussed before. So in case (c) the color varies continuously as strings overlap. In general the multiplicity of a cluster of n strings is now given by

$$\mu_n = \sqrt{n\frac{A_n}{A_1}}\mu_1(E). \tag{4.13}$$

To calculate the chaoticity parameter we proceeded as in case (b) but changing formula (4.12) to (4.13). The results are plotted in Fig. 4 for the same collisions as in (b). The error bars correspond to the statistics of the simulation. It is seen that the η scaling is essentially recovered.

Also at high η, λ reaches higher values than in the previous case.

5 Conclusions

The systematic determination of the chaoticity parameter can provide valuable information on the possibility of collective phenomena in nucleus–nucleus collisions. In this paper we studied different scenarios of the interaction between color strings, comparing their predictions for the chaoticity parameter with the experimental data. The no-interaction (independent strings) scenario and string fusion scenario with the fused string having the same transverse area as its parents seem to be excluded by the data. In the percolation scenario different dynamical possibilities were studied with a different distribution of the color field inside the cluster. We find that the cases where each cluster acts like a single chaotic source are in agreement with the experimental data. Case (c) of the percolation, when the multiplicity suppression is controlled by the area of the cluster, looks especially attractive. In this case for $\eta > 0.5$ the shape of the chaoticity parameter as a function of η is very similar to the dependence of the fractional average cluster size, and at the critical point, $\eta = \eta_c$, $\mathrm{d}\lambda/\mathrm{d}\eta$ has a maximum.

A systematical experimental study of this possibility in the SPS, RHIC and LHC forthcoming experiments would be welcome.

Acknowledgements. This work has been done under contracts AEN99-0589-C02 of Spain, PGIDTOOPXI20613PN of Xunta de Galicia and NATO grant PST.CLG.976799. F.d.M. thanks Xunta de Galicia for a fellowship. We thank N. Armesto and D. Sousa for computational help and comments. We thank J. Seixas for asking a question in which this work originates, and B. Andersson, A. Giovannini and P. Seyboth for discussions.

References

1. R. Hanbury-Brown, R.Q. Twiss, Nature **178**, 1046 (1956)
2. G. Goldhaber, S. Goldhaber, W. Lee, A. Pais, Phys. Rev. **120**, 300 (1960)
3. U.A. Wiedemann, U. Heinz, Phys. Rep. **319**, 145 (1999)
4. S. Pratt, Phys. Rev. D **33**, 72 (1986); Phys. Rev. C **49**, 2722 (1994)
5. R. Weiner, Introduction to Bose–Einstein correlations and subatomic interferometry (John Wiley, 2000); Phys. Rep. **327**, 249 (2000)
6. T. Csörgő, hep-ph/0001233
7. M.I. Podgoretskii, Sov. J. Nucl. Phys. **37**, 272 (1983)
8. G.N. Fowler, R.M. Weiner, Phys. Rev. D **17**, 3118 (1978)
9. M. Gyulassy, S.K. Kauffmann, L.W. Wilson, Phys. Rev. C **20**, 2267 (1979)
10. B. Andersson, W. Hofmann, Phys. Lett. B **169**, 364 (1986)
11. B. Andersson, M. Ringner, Nucl. Phys. B **513**, 627 (1998)
12. B. Andersson, The Lund model (Cambridge University Press, 1998)
13. B. Andersson, Rencontres de Moriond 2000; J. Häkkinen, M. Ringner, Eur. Phys. J. C **5**, 275 (1998)
14. E.A. De Wolf, hep-ph/0101243
15. A. Capella, A. Krzywicki, E. Levin, Phys. Rev. D **44**, 704 (1991)
16. J.A. van Dalen, Proceedings of the IX Int. Workshop on Multiparticle production, Nucl. Phys. B (Proc. Suppl.) **92**, 247 (2001); R. Barate et al., Phys. Lett. B **478**, 50 (2000); M. Aciarri et al., Phys. Lett. B **493**, 23 (2000)
17. A. De Angelis, L. Vitale, Proceedings of the IX International Workshop on Multiparticle production, Nucl. Phys. B (Proc. Suppl.) **92**, 259 (2001); O. Smirnova, Proceedings of the IX International Workshop on Multiparticle production, Nucl. Phys. B (Proc. Suppl.) **92**, 301 (2001)
18. M. Biyajima, N. Suzuki, G. Wilk, Z. Wlodarczyk, Phys. Lett. B **386**, 297 (1996); M. Biyajima, Prog. Theor. Phys. **69**, 966 (1983); Phys. Lett. B **137**, 225 (1984)
19. A. Giovannini, G. Veneziano, Nucl. Phys. B **130**, 61 (1977)
20. A. Breakstone et al., Z. Phys. C **33**, 333 (1987); C. Albajar et al., UA1 Collaboration, Phys. Lett. B **226**, 410 (1989); B. Buschbeck, H.C. Eggers, P. Lipa, Phys. Lett. B **481**, 187 (2000)
21. G. Alexander, E. Sarkisyan, hep-ph/0005212
22. WA80 Collaboration, R. Albrecht et al., Z. Phys. C **53**, 225 (1992)
23. WA80 Collaboration, T.C. Awes et al., Z. Phys. C **69**, 67 (1995)
24. NA44 Collaboration, H. Beker et al., Phys. Rev. Lett. **74**, 3340 (1995); NA44 Collaboration, G. Bearden et al., Phys. Rev. C **58**, 1656 (1998)
25. NA44 Collaboration, M. Bøggild et al., Phys. Lett. B **302**, 510 (1993)
26. W.A. Zadjc et al., Phys. Rev. C **29**, 2173 (1984)
27. M.G. Bowler, Z. Phys. C **29**, 617 (1985); Phys. Lett. B **276**, 237 (1992)
28. N.S. Amelin, M.A. Braun, C. Pajares, Phys. Lett. B **306**, 312 (1993); Z. Phys. C **63**, 507 (1994)
29. H. Sorge, Phys. Rev. C **52**, 3291 (1995)
30. M.A. Braun, C. Pajares, Nucl. Phys. B **390**, 542 (1993); Nucl. Phys. B **390**, 559 (1993); Phys. Lett. B **287**, 154 (1992)
31. M.A. Braun, C. Pajares, J. Ranft, J. Mod. Phys. A **14**, 2689 (1999)
32. N. Armesto, M.A. Braun, E.G. Ferreiro, C. Pajares, Phys. Rev. Lett. **77**, 3736 (1996)
33. J. Dias de Deus, R. Ugoccioni, A. Rodrigues, Eur. Phys. J. C **16**, 537 (2000)
34. M.A. Braun, C. Pajares, Eur. Phys. J. C **16**, 349 (2000)
35. M. Nardi, H. Satz, Phys. Lett. B **442**, 14 (1998); H. Satz, Nucl. Phys. A **642**, 130c (1998); Nucl. Phys. A **661**, 104c (1999)